ELSEVIER

Polymer 43 (2002) 6073–6084

polymer

www.elsevier.com/locate/polymer

Poly(ester amide)s derived from 1,4-butanediol, adipic acid and 1,6-aminohexanoic acid: characterization and degradation studies

Emma Botines, Alfonso Rodríguez-Galán, Jordi Puiggalí*

Departament d'Enginyeria Química, E.T.S. d'Enginyers Industrials, Universitat Politècnica de Catalunya, Av. Diagonal 647, E-08028 Barcelona, Spain

Received 21 May 2002; received in revised form 22 July 2002; accepted 11 August 2002

Abstract

The commercial biodegradable copolymer BAK 1095 has been studied by means of spectroscopy, X-ray diffraction and calorimetry. Degradability has been evaluated in different media (hydrolytic at distinct temperatures and pHs, and enzymatic) by evaluating the changes in intrinsic viscosity, in the NMR spectra, in mechanical properties and in the surface texture of samples. In addition, a new poly(ester amide) with a regular distribution of the monomers implied in BAK 1095 has also been synthesized and its characteristics compared with the reference polymer. © 2002 Published by Elsevier Science Ltd.

Keywords: Degradability; Poly(ester amide)s; BAK 1095

1. Introduction

Poly(ester amide)s constitute a new series of thermoplastic polymers that can combine a high technical performance with a good biodegradability. In this sense, Bayer has recently produced the BAK 1095 and BAK 2195 polymers, which appear to have a wide range of applications as biodegradable materials [1]. The first one is a statistical polymer based on 1,4-butanediol, adipic acid and 1,6-aminohexanoic acid and is the main subject of this work. For the sake of completeness, a new polymer characterized by a regular distribution of the above-mentioned monomers has been synthesized and its properties compared with the commercial polymer. Furthermore, the new poly(ester amide) is related to other sequential polymers previously studied by us [2–5], which were composed of natural amino acids instead of 1,6-aminohexanoic acid units. PAHBAH4 will be used to name the polymer based on the sequence: $-[NH(CH_2)_5CO-O(CH_2)_4O-CO(CH_2)_5NH-CO(CH_2)_4CO]-$ (P, AH, B and 4 for polymer, 1,6-aminohexanoic acid, 1,4-butanediol and the dicarboxylic acid of 4 methylene groups, respectively).

2. Experimental part

2.1. Synthesis

All chemicals were ACS grade and used without further purification. BAK 1095 was kindly supplied by Bayer Hispania S.A., whereas nylon 6 was purchased from Aldrich. PAHBAH4 was synthesized according to the thermal polyesterification method previously established for some glycine derivatives and outlined in Scheme 1. Polyester 4 6 was obtained from adipic acid and an excess of 1,4-butanediol (molar ratio: 2.2/1) by thermal polycondensation in vacuum at 185 °C and using titanium butoxide as catalyst.

2.2. Characterization

Intrinsic viscosities were determined with a Cannon-Ubbelohde microviscometer in dichloroacetic solutions at 25 ± 0.1 °C.

Infrared absorption spectra were recorded with a Perkin–Elmer 1600 FT-IR spectrometer in the 4000–500 cm^{-1} range from films prepared from evaporation of formic acid solutions. NMR spectra of polymers were registered from deuterated chloroform/trifluoroacetic acid solutions. Chemical displacements were calibrated using tetramethylsilane as an internal standard. A Bruker AMX-300

* Corresponding author. Fax: +34-934017150.
E-mail address: puiggali@eq.upc.es (J. Puiggalí).

0032-3861/02/$ - see front matter © 2002 Published by Elsevier Science Ltd.
PII: S0032-3861(02)00577-3

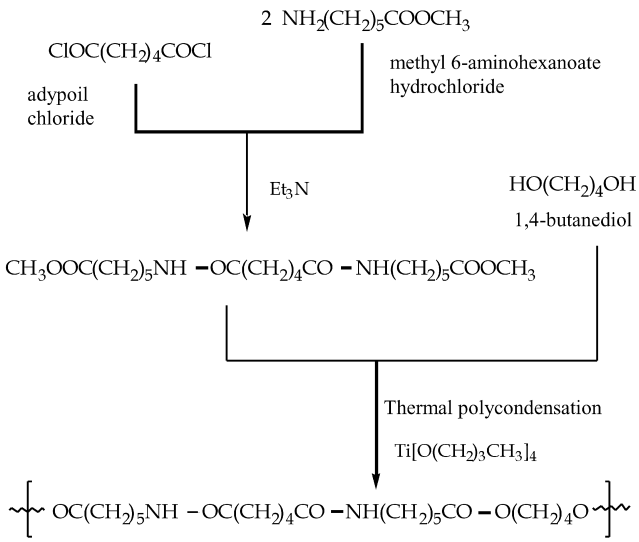

Scheme 1.

spectrometer operating at 300.1 and 75.5 MHz was used for ^{1}H and ^{13}C NMR investigations, respectively.

Thermal analysis was performed by differential scanning calorimetry with a Perkin–Elmer DSC-PYRIS 1, using indium metal for calibration. Thermogravimetric analysis was carried out with a Perkin–Elmer TGA-6 thermobalance. Heating and cooling runs were performed under a flow of dry nitrogen at 20 and 10 °C/min, respectively.

Dynamic–mechanical behavior was analyzed using a Rheometrics PL-DMT MK3 instrument. Work frequency was 1 Hz. After a rapid cooling, the dynamic spectrum was detected on heating the sample at 2 °C/min in the temperature range −150 to 120 °C. Complex modulus and tan δ were obtained and reported as a function of temperature. In this case, samples of 2.5 cm × 1 cm were cut off from films with a thickness of 450 μm prepared by melt pressing.

Fiber X-ray diffraction patterns were recorded in vacuum at room temperature. Calcite ($d_B = 3.035$ Å) was used for calibration. A modified Statton camera (W.H. Warhus, Wilmington, DE) with a nickel-filtered radiation of 1.542 Å was used for these experiments.

Samples for mechanical and degradation studies were cut off from regular films of 200 μm of thickness prepared by melt pressing 200 mg of the appropriate polymer at a temperature of 10 °C below fusion. Plate samples with a length of 30 mm and a width of 3 mm were used for the evaluation of mechanical properties, whereas plates of 15 mm × 15 mm were usually employed in the degradation experiments.

Mechanical properties were determined with a Zwick Z2.5/TN1S testing machine in stress–strain experiments, which were carried out at a deformation rate of 10 mm/min. Mechanical parameters were averaged from a minimum of 10 measurements for each polymer sample.

Hydrolytic degradation assays were carried out in a pH 7.4 sodium phosphate buffer. Each plate was kept in a bottle filled with 30 ml of the buffer and sodium azide (0.03 wt%) to prevent microbial growth. After the immersion time, the retrieved samples were thoroughly rinsed with distilled water. Wet samples for mechanical measurements were obtained after absorption of superficial water with a filter paper. The remaining samples were dried to constant weight in vacuum, and stored over $CaCl_2$ before analysis. Hydrolysis was also studied under accelerated conditions provided by: (a) distilled water at a temperature of 70 °C, (b) a pH 2.3 sodium citrate buffer at 37 °C, (c) a pH 10.5 sodium carbonate buffer at 37 °C. Degradation was also evaluated in: (a) activated sludges from a purifying plant, which were renewed every 15 days, and (b) a medium consisting of a pH 7.4 sodium phosphate buffer with 0.5 > vol% of the activated sludges.

Enzymatic degradation studies were conducted at 37 °C by using lipases from *Pseudomonas cepacia* (LPC), *Candida cylindracea* (LCC) or *Rhizopus arrhizus* (LRA), or proteolytic enzymes such as papain, proteinase K or chymotrypsin. The enzymatic media, 10 ml, consisted of a sodium phosphate buffer (pH 6.0 for papain and 7.4 for the other enzymes) containing sodium azide (0.03 wt%) and 1 mg of the appropriate enzyme. In the case of papain, the solution also contained L-cysteine (34 mM) and ethylenediaminetetracetic disodium salt (30 mM) for activation. All enzymatic solutions were renewed every 72 h because of enzymatic activity loss. After the immersion time, the retrieved samples were immersed in a HCl solution, rinsed with water, and dried as indicated for hydrolytic experiments.

Mass loss, intrinsic viscosity, changes in NMR spectra and mechanical properties were evaluated in these hydrolytic and enzymatic degradation studies.

Scanning electron microscopy was employed to examine the changes in the texture of samples after degradation. Gold coating was accomplished by using a Balzers SCD-004 Sputter Coater. The SEM micrographs were carried out with a JEOL JSM-6400 instrument.

3. Results and discussion

3.1. Synthesis of PAHBAH4

3.1.1. N,N′-Bis(methoxycarbonylpentamethylene) adipamide

A round bottom flask equipped with a dropping funnel and a magnetic stirrer was purged with N_2 and charged with methyl 6-aminohexanoate hydrochloride (0.04 mol), triethylamine (0.08 mol) and 50 ml of chloroform. Then, 0.02 mol of adipoyl chloride dissolved in 20 ml of chloroform were slowly added for 90 min, while the reaction was kept at 0 °C by means of an ice water bath. The reaction was prolonged for an additional period of 3 h at room temperature. The chloroform solution was extracted with 3 × 15 ml of water, dried with anhydrous sodium sulphate,

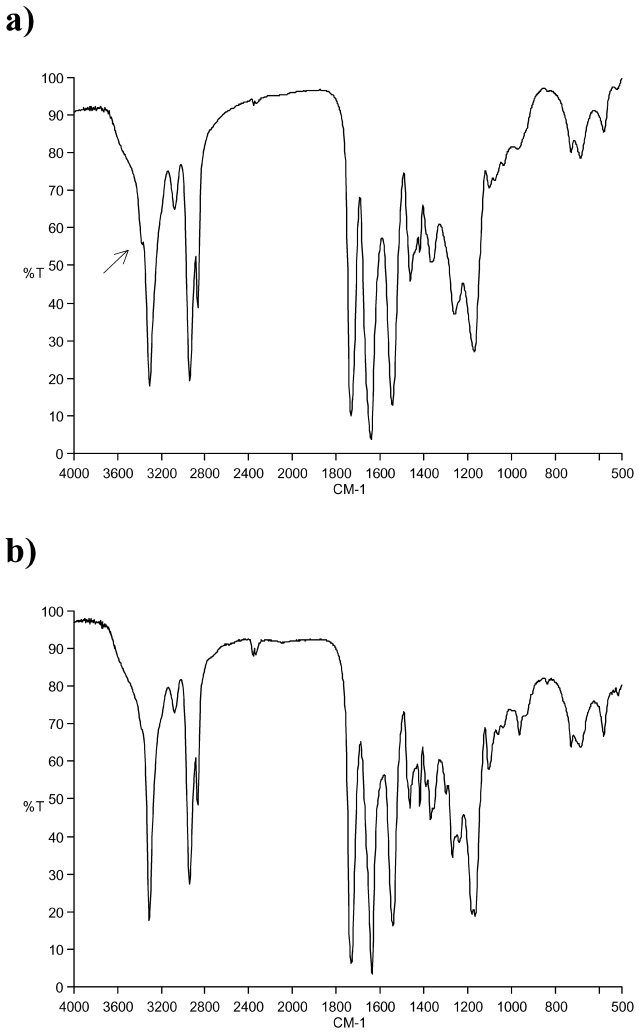

Fig. 1. Infrared spectra of BAK 1095 (a) and PAHBAH4 (b). Note the shoulder in the amide A band (indicated by an arrow) of BAK 1095.

filtered and evaporated under reduced pressure. The resulting solid was washed with ethyl ether and recrystallized from methanol/water (1/1, v/v). Yield: 47%; mp: 122 °C.

^{1}H NMR ($CDCl_3$, TMS, int. ref.): δ 5.94 (m, 2H, NH), 3.67 (s, 6H, CH_3), 3.24 (m, 4H, CH_2NH), 2.32 (t, 4H, OCOCH_2), 2.22 (t, 4H, NHCOCH_2), 1.82 (m, 4H, CH_2CH$_2$NH), 1.65 (m, 4H, OCOCH$_2$CH_2), 1.55 (m, 4H, NHCOCH$_2$CH_2), 1.35 (m, 4H, OCOCH$_2$CH$_2$CH_2).

Ana. calcd for $C_{20}H_{36}N_2O_6$: C, 60.00%; H, 9.00%; N, 7.00%. Found: C, 59.85%; H, 9.07%; N, 7.05%.

3.1.2. Thermal polyesterification

A two-neck, round bottom flask equipped with a magnetic stirrer and a condenser was charged with 1,4-butanediol (0.025 mol) and *N*,*N*′-bis(methoxycarbonylpentamethylene)adipamide (0.01 mol). Titanium butoxide was also added as a catalyst for condensation reaction. The flask was heated in an oil bath at 150 °C in order to melt the mixture. Meanwhile, a slow stream of nitrogen was passed

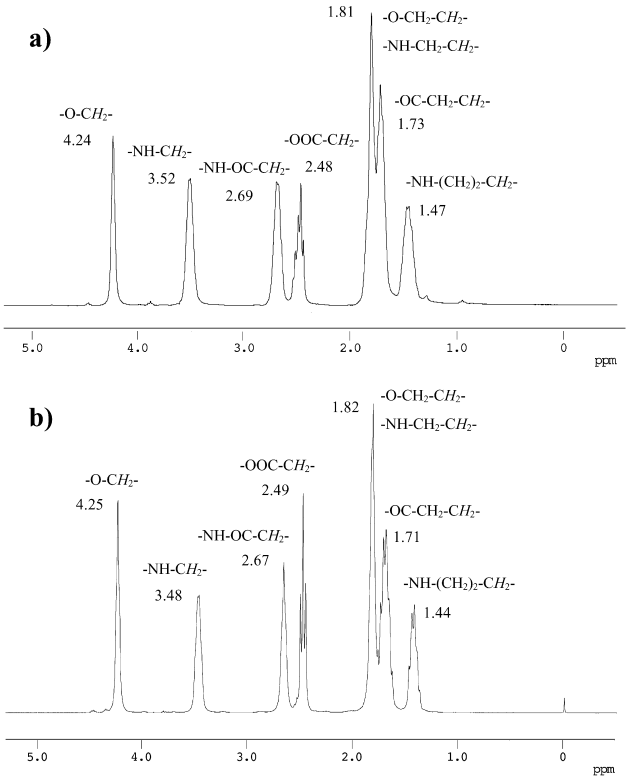

Fig. 2. ^{1}H NMR spectra of BAK 1095 (a) and PAHBAH4 (b) with assignment of the main peaks. Note the increase in the ratio area of peaks associated to ester linkages for PAHBAH4 sample.

to help eliminate the methanol and the excess of diol. After 1 h, the second neck was connected to a vacuum pump (0.3 mm Hg) while the temperature of the bath was raised to 180 °C. In order to improve the elimination of the diol, the reaction was periodically stopped (every 2 h) by cooling it to room temperature, and then the diol that had condensed in the flask wall was removed. The reaction was prolonged until no more diol was distilled off (12 h). After cooling down, the polymer was dissolved in a mixture of formic acid/TFA (9/1, v/v), precipitated by a dropwise addition of methanol, filtered and repeatedly washed with ethyl ether.

3.2. Characterization

The intrinsic viscosity of PAHBAH4, measured in dichloroacetic acid, is comparable to that found for the commercial sample of BAK 1095: 0.88 and 1.04 dl/g, respectively. In addition, values of 0.91 and 0.60 dl/g were determined for the synthesized polyester 4 6 and the commercial nylon 6, respectively.

The infrared spectrum of BAK 1095 shows the characteristic absorption bands of methylene (2936 and 2863 cm^{-1}), ester (1730 cm^{-1}), and amide groups (3305, 3084, 1644 and 1549 cm^{-1}). It should be pointed out that the amide A band (NH stretching mode) appears with a shoulder at 3380 cm^{-1} (Fig. 1), which suggests the existence of some weaker hydrogen bond interaction like

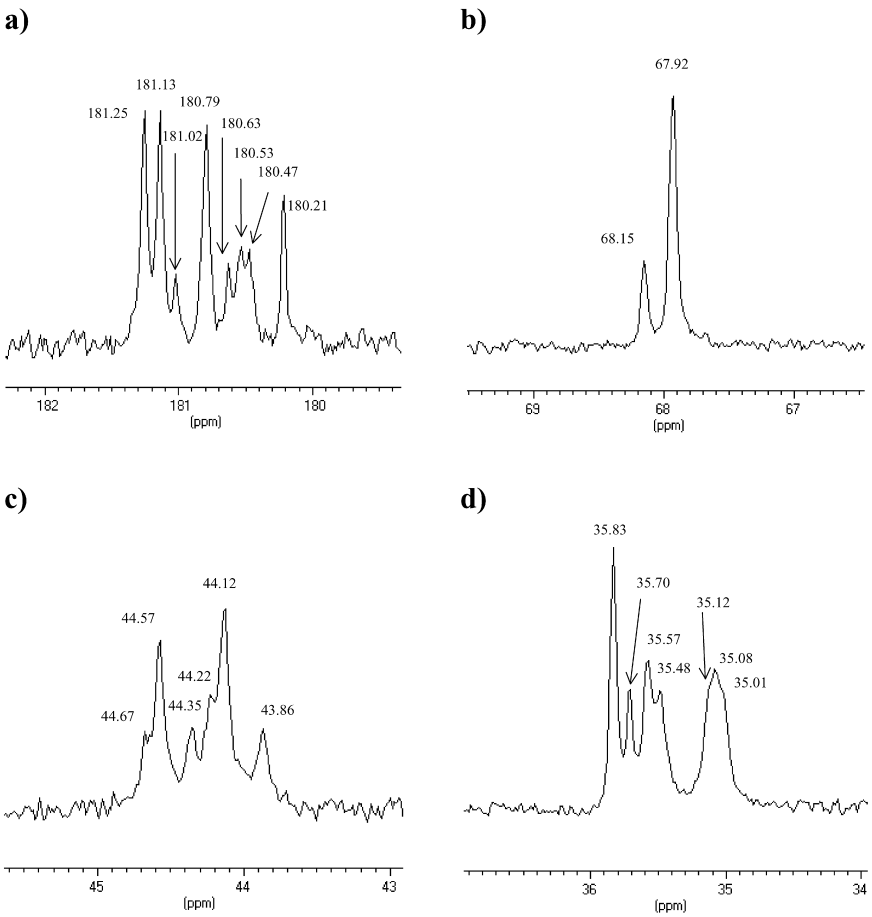

Fig. 3. ^{13}C NMR spectra of BAK 1095 showing zones associated to CO (a), CH_2-O (b), CH_2-NH (c) and CH_2-CO (d) carbons.

that established between the hydrogen of the amide group and the carbonyl oxygen of the ester group. In this sense, the ester, amide I and amide II bands appear broad and contrast with the finer bands observed in the spectrum of the ordered PAHBAH4 sample (main absorptions at 3307, 2939, 2864, 1732, 1636 and 1548 cm^{-1}). Crystallographic studies of some model compounds indicate that like to like amide–amide hydrogen bonds can coexist with the like to unlike

Table 1
Chemical shifts and assignments of the ^{13}C NMR spectra of BAK 1095

Sequence	Chemical displacement (ppm)				Ratio area (%)	
	BAK 1095	Nylon 6	PAHBAH4	Polyester 4 6	BAK 1095	Random polymer
$\cdots C H_2O-CO(CH_2)_5NH-CO\cdots$	68.15				24	24
$\cdots C H_2O-CO(CH_2)_4CO-O\cdots$	67.92			67.92	76	16
$\cdots C H_2O-CO(CH_2)_4CO-NH\cdots$	67.92		67.92		76	60
$\cdots O-CO(CH_2)_4C H_2NH-CO(CH_2)_4CO-O\cdots$	44.67				9	6.4
$\cdots O-CO(CH_2)_4C H_2NH-CO(CH_2)_5NH-CO\cdots$	44.57				25	24
$\cdots O-CO(CH_2)_4C H_2NH-CO(CH_2)_4CO-NH\cdots$	44.35		44.35		12	9.6
$\cdots NH-CO(CH_2)_4C H_2NH-CO(CH_2)_4CO-O\cdots$	44.22				10	9.6
$\cdots NH-CO(CH_2)_4C H_2NH-CO(CH_2)_5NH-CO\cdots$	44.12	44.12			30	36
$\cdots NH-CO(CH_2)_4C H_2NH-CO(CH_2)_4CO-NH\cdots$	43.86				14	14.4
$\cdots CO-NH(CH_2)_4C H_2CO-O\cdots$	35.83		35.83		25	24
$\cdots O-CO(CH_2)_3C H_2CO-O\cdots$	35.70			35.70	8	8.2
$\cdots CO-NH(CH_2)_4C H_2CO-NH(CH_2)_5CO-NH\cdots$	35.57	35.57			25	22
$\cdots CO-NH(CH_2)_4C H_2CO-NH(CH_2)_5CO-O\cdots$	35.48				15	14
$\cdots NH-CO(CH_2)_3C H_2CO-O\cdots$	35.12				7	6.3
$\cdots O-CO(CH_2)_3C H_2CO-NH\cdots$	35.08				18	6.3
$\cdots NH-CO(CH_2)_3C H_2CO-NH(CH_2)_5CO-NH\cdots$	35.08				18	11.1
$\cdots NH-CO(CH_2)_3C H_2CO-NH(CH_2)_5CO-O\cdots$	35.01		35.01		12	7.4

ester–amide interactions [6,7], a fact also compatible with theoretical investigations [8].

Analysis of the ^{1}H NMR spectrum gives the composition ratio of BAK 1095. According to the assignment given in Fig. 2(a), the area of the two signals observed at 4.24 and 3.52 ppm can be used to obtain the butanediol (B) and aminohexanoic acid (AH) content, respectively. Note that the number of butanediol and adipic residues (A) must be the same, and consequently:

$$\%B = \%A = (A_{4.24}/4)/[2 \times (A_{4.24}/4) + (A_{3.52}/2)] \times 100$$

$$\%AH = (A_{3.52}/2)/[2 \times (A_{4.24}/4) + (A_{3.52}/2)] \times 100$$

The sample of BAK 1095 is composed of approximately 60% of aminohexanoic residues and 20% of both butanediol and adipic units, which implies an amide–ester ratio of 60/40. This fact allows the two signals observed at 2.69 and 2.48 ppm to be assigned to the methylene protons close to the carbonyl of an amide and an ester group, respectively, since their area ratio ($A_{2.69}/A_{2.48}$) is approximately 6/4.

The analysis of the ^{1}H NMR spectrum of PAHBAH4 (Fig. 2(b)) indicates 50% of amide and ester linkages, as expected.

^{13}C NMR of BAK 1095 shows multiple and intense signals for the CO, CH_2–O, CH_2–NH and CH_2–CO carbons (Fig. 3), suggesting a random distribution of monomers. Thus, there is no evidence of long blocks constituted by nylon 6 ($-[NH(CH_2)_5CO]_x-$) or polyester 4 6 ($-[O(CH_2)_4OCO(CH_2)_4CO]_y-$) sequences. Spectra were registered with a delay time between pulses sufficiently high to suppose that all carbons were relaxed, and consequently the area of signals could be directly used to determine sequence distribution. Deconvolution of signals was performed with the WINNMR program. Table 1 shows the observed displacements and the proposed assignment for methylene carbons. NMR spectra of BAK 1095 plus Nylon 6, Polyester 4 6 or PAHBAH4 were also registered in order to associate the observed peaks to a given sequence. The indicated polymers were used as internal references, since chemical displacements were slightly sensitive to the TFA/chloroform ratio.

Table 1 clearly shows that the experimental content of the different sequences is close to the theoretical values expected for a statistical distribution of the monomers taking into account their chemical restrictions (i.e. a butanediol unit cannot be linked to the amine group of aminohexanoic acid).

Signals near 68 ppm (attributed to the CH_2–O carbon atom of a butanediol unit) appear split due to neighboring-group effects. Three different sequences may be considered: B–AH, B–A–B and B–A–AH. However, the data on Polyester 4 6 (B–A–B sequence) and PAHBAH4 (B–AH sequence) indicate that the former cannot be differentiated, and therefore only two signals are expected in the NMR spectra. Note also that the diad B–AH cannot be split into the two possible triads B–AH–A and B–AH–AH due to the fact that chemical differences are found beyond 14 main chain atoms. This is not the case of the B–A diad, since differences appear after only seven atoms. Statistical probabilities of 60 and 40% can be assigned to the B–AH and B–A diads, respectively, taking into account the composition of the polymer. In the same way, the two triads B–A–B and B–A–AH correspond to 40 and 60% of the B–A diad.

The methylene adjacent to the NH group (AH unit) appears approximately at 44 ppm and is split into two groups of three signals. The groups are associated to the diads B–AH and AH–AH, since chemical differences are found after only five atoms in the direction of the preceding monomer. Note also that the rear monomers produce chemical differences after six or seven atoms. Thus, the sequences AH–A–B, AH–A–AH and AH–AH give rise to the three signal splitting. As confirmation of the random distribution of BAK 1095, a number-average length (L) of 2.17 for a nylon 6 block can be evaluated according to the percentage of the B–AH diad: L (AH) = 100/%B–AH.

Much more complicated is the assignment of signals corresponding to the methylene adjacent to a carbonyl group that appears near 35 ppm and that can belong either to an aminohexanoic or an adipic unit. As a general trend, sequences with ester groups move downfield with respect to similar ones constituted by amide groups. This fact, together with the displacements deduced from the reference polymers (four sequences), allows the assignment given in Table 1 to be proposed.

3.2.1. Thermal behavior

The calorimetric analysis of BAK 1095 and PAHBAH4 consisted of four DSC scans, as shown in Fig. 4. In order to have controlled starting conditions, the commercial BAK 1095 sample was precipitated by dropwise addition of its solution in a formic/trifluoroacetic acid (9:1, v/v) mixture into ether, and then annealed for 1 h at 110 °C. In the first run, the initial samples were heated through fusion and left in the melt state for 2 min. Subsequent cooling was performed to observe crystallization from the melt. A second heating was carried out to check the reproducibility of the transitions and to obtain data for the melt-crystallized samples. In order to determine the glass transition temperatures, a third heating run was performed with samples quenched from the melt state. Heats of fusion were used to evaluate the crystallinity of polymers (solution- and melt-crystallized samples) taking into account the heats of fusion for 100% crystalline materials. These values were estimated from the reported [9] group contributions of ester (−2.5 kJ/mol), amide (2.0 kJ/mol) and methylene (4.0 kJ/mol). Temperatures indicative of the beginning of the decomposition process ($T_{d,0}$) and the 50% weight loss ($T_{d,1/2}$) were determined by thermogravimetry. Table 2 summarizes the main calorimetric parameters of the studied polymers. The following considerations can be remarked on:

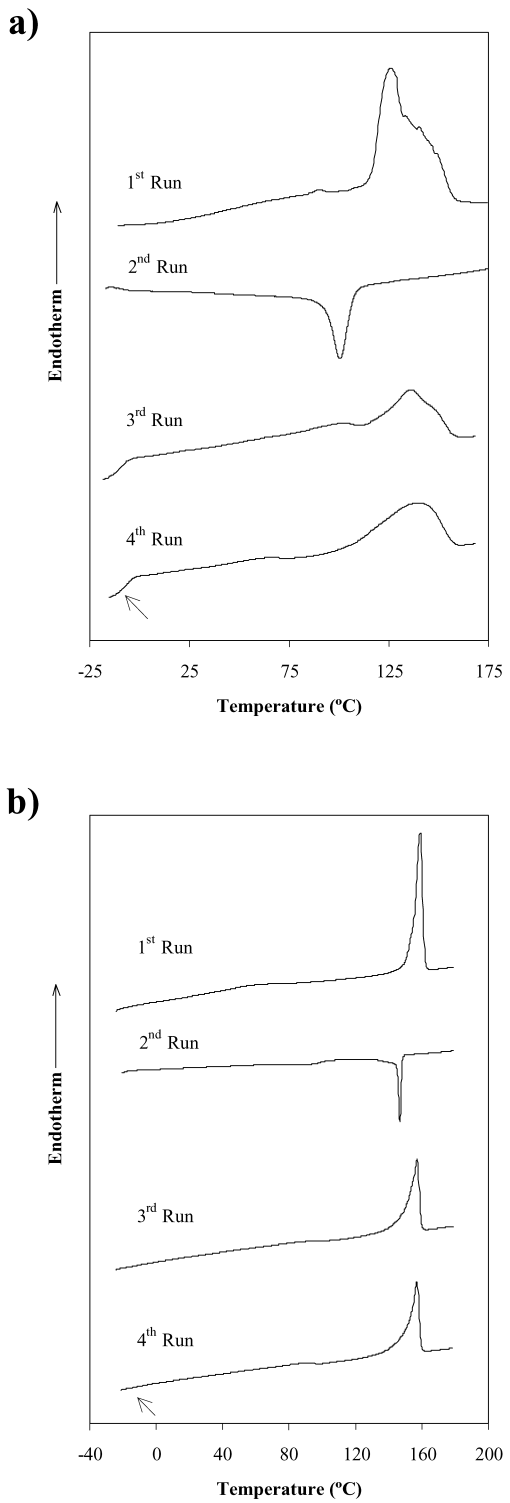

Fig. 4. Sequence of the four DSC scans performed with BAK 1095 (a) and PAHBAH4 (b) samples. Arrows indicate glass transition temperatures.

1. The statistical monomer distribution of BAK 1095 precludes its solution crystallization in the assayed conditions. An appreciable melting peak was only observed after the annealing treatment.
2. In spite of its lower amide content, the PAHBAH4 sample melts at a higher temperature than BAK 1095. Crystallization also occurs at a higher temperature indicating that a lower supercooling is needed to crystallize the sample. The estimated values for the degree of crystallinity are also in agreement with the expected higher crystallinity of the ordered polymer. A recovery in crystallinity close to 70% for the melt-crystallized sample, compared to the original solution-crystallized PAHBAH4 sample, was observed.
3. Glass transition temperatures of poly(ester amide)s are close to −15 °C and intermediate between those expected for polyester 4 6 (−50 °C) and nylon 6 (40–87 °C) [10].
4. The melt processing of poly(ester amide)s is not hindered, since they are stable through fusion. Comparison of decomposition temperatures indicates a similar stability for both polymers, although the regular polymer starts to decompose at a lower temperature. Thus, a 1.3% weight loss is observed for the PAHBAH4 sample when the $T_{d,0}$ temperature of BAK 1095 is reached. In the same way, isothermal thermogravimetries performed at 300 °C indicate a weight loss close to 25 and 23% for PAHBAH4 and BAK 1095 samples, respectively, after 2 h.

Dynamic–mechanical behavior was also studied to determine glass transition temperatures (Fig. 5). Both

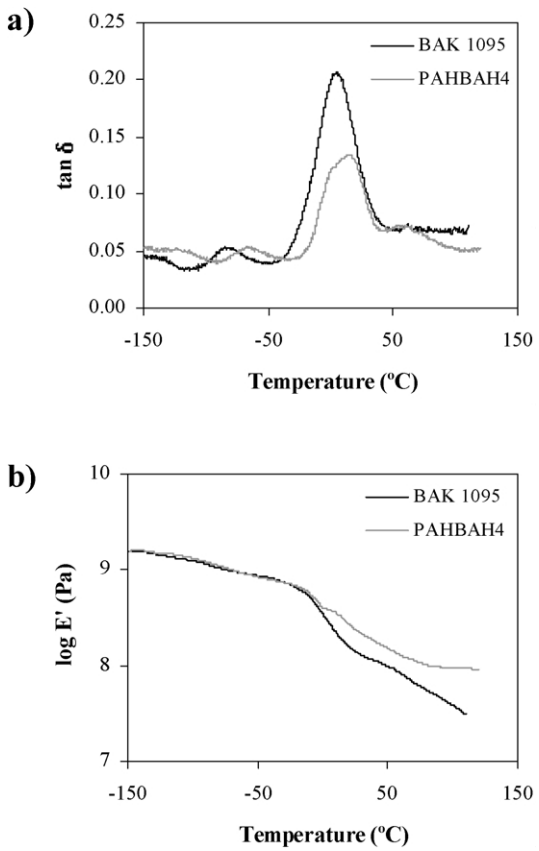

Fig. 5. (a) Loss term tan δ as a function of temperature for the BAK 1095 and PAHBAH4 poly(ester amide)s. (b) Storage modulus E' reported as a function of temperature for indicated poly(ester amide)s.

Table 2
Main calorimetric data of the polymers studied in this work

Polymer	1st Run			2nd Run		3rd Run			4th Run			Thermogravimetry	
	T_m[a] (°C)	ΔH_f[a] (kJ/mol)	χ (%)[a,b]	T_c (°C)	ΔH_c (kJ/mol)	T_m (°C)	ΔH_f (kJ/mol)	χ (%)[b]	T_g (°C)	T_m (°C)	ΔH_f (kJ/mol)	$T_{d,0}$ (°C)	$T_{d,1/2}$ (°C)
BAK 1095	126	5.7	30	101	2.9	136	2.6	14	−11	139	2.6	352	427
PAHBAH4	159	30.1	42	147	19.2	157	22.7	32	−15	157	22.4	291	430

[a] The sample was previously annealed at 110 °C for 1 h.
[b] Crystallinity evaluated assuming 19.1 and 71 kJ/mol as the heat of fusion for 100% crystalline samples of BAK 1095 and PAHBAH4. The molecular weight of a PAHBAH4 and a statistical BAK 1095 repeat units were 426 and 108 g/mol, respectively.

BAK 1095 and PAHBAH4 polymers show a narrow dissipation band in the tan δ function and a sudden decrease of the storage modulus E'. This feature is an indication of well defined glass transitions that occur at temperatures close to −5 °C, in good agreement with the DSC calorimetric results. The transition is more remarkable for the BAK 1095 sample with a higher amorphous content. A β transition, Schatzki's crankshaft motion, close to −90 and −65 °C, can also be determined for BAK 1095 and PAHBAH4 samples, respectively.

3.3. X-ray diffraction

X-ray fiber patterns of BAK 1095 (Fig. 6(a)) show very broad and diffuse reflections, indicative of small crystalline domains. The main equatorial reflections correspond to 4.42 and 3. 72 Å, which are close to the characteristic values of nylon 6 [11]. Thus, the chain packing rests on a stacking of hydrogen bonded sheets (intrachain distance of 4.79 Å and intersheet spacing of 3.72 Å), which are shifted by approximately 4.79/3 Å along the hydrogen bonding direction. The appearance of some weak off-meridional reflections indicating a chain axis periodicity close to 8.2 Å, a lower value than the 17.2/2 Å characteristic of nylon 6, is

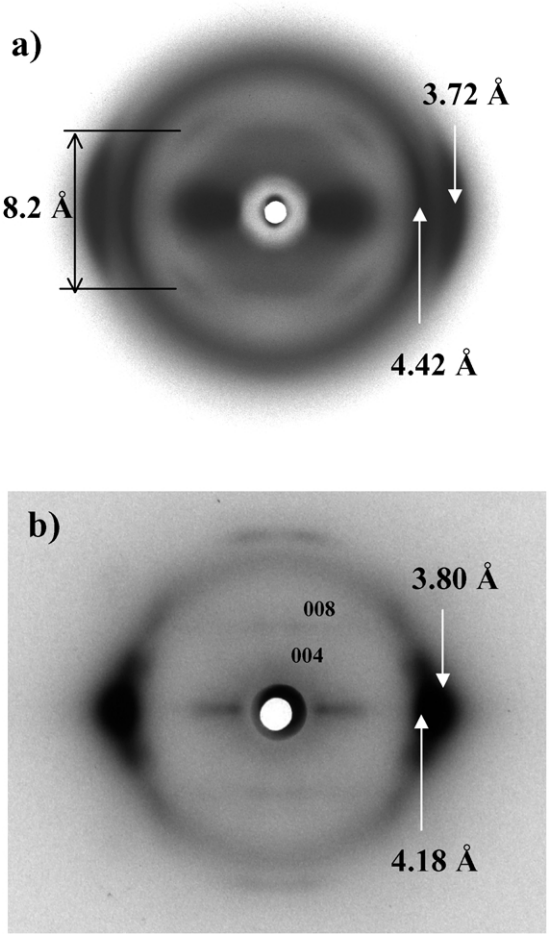

Fig. 6. Fiber X-ray diffraction patterns of BAK 1095 (a) and PAHBAH4 (b). Main reflections are indicated by arrows.

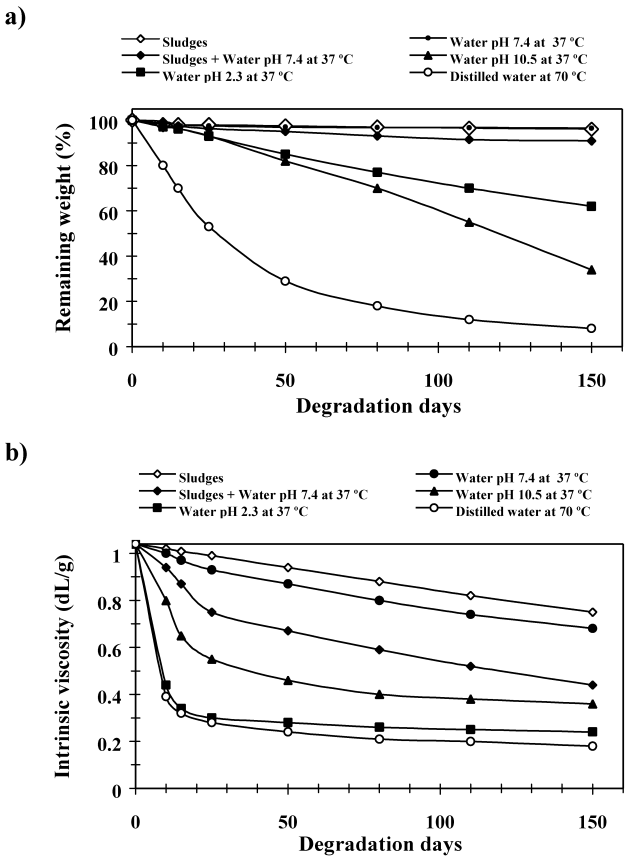

Fig. 7. Remaining weight percentages (a) and intrinsic viscosities (b) of BAK 1095 samples exposed to different hydrolytic degradation media.

Table 3
Remaining weight (%) of BAK 1095 samples exposed to different enzymatic media after the indicated periods of incubation

Time (days)	Lipase from *P. cepacia*	Lipase from *C. cylindracea*	Lipase from *R. arrhizus*	Papain	Proteinase K	Chymotrypsin
3	99	99	99	99.5	94	99.5
9	98	98	98	99	80	99
15	98	98	97	98	72	98
21	97	97	96	97	68	97

also remarkable. This fact, together with both the statistical distribution, found in NMR analysis and the absence of a T_g associated to polyamide blocks in calorimetric studies, suggests a crystallographic repeat related to the average spacing between carbonyl groups. Note that they are responsible for the main differences in electronic density along the molecular chain, and that a value close to 8.25 Å is expected for a fully extended conformation. This value is calculated according to the expression $0.6 \times 8.75 + 0.2 \times 8.75 + 0.2 \times 6.25$, where 8.75 Å is the distance between carbonyls separated by an aminohexanoic or a butanediol unit, and 6.25 Å corresponds to the distance between the carbonyls of an adipic residue.

Fiber patterns of PAHBAH4 (Fig. 6(b)) show a higher crystallinity than those of BAK 1095 and a packing mode similar to that described for related poly(ester amide)s [4] constituted by glycine units instead of aminohexanoic residues. Thus, the two strong equatorial reflections at

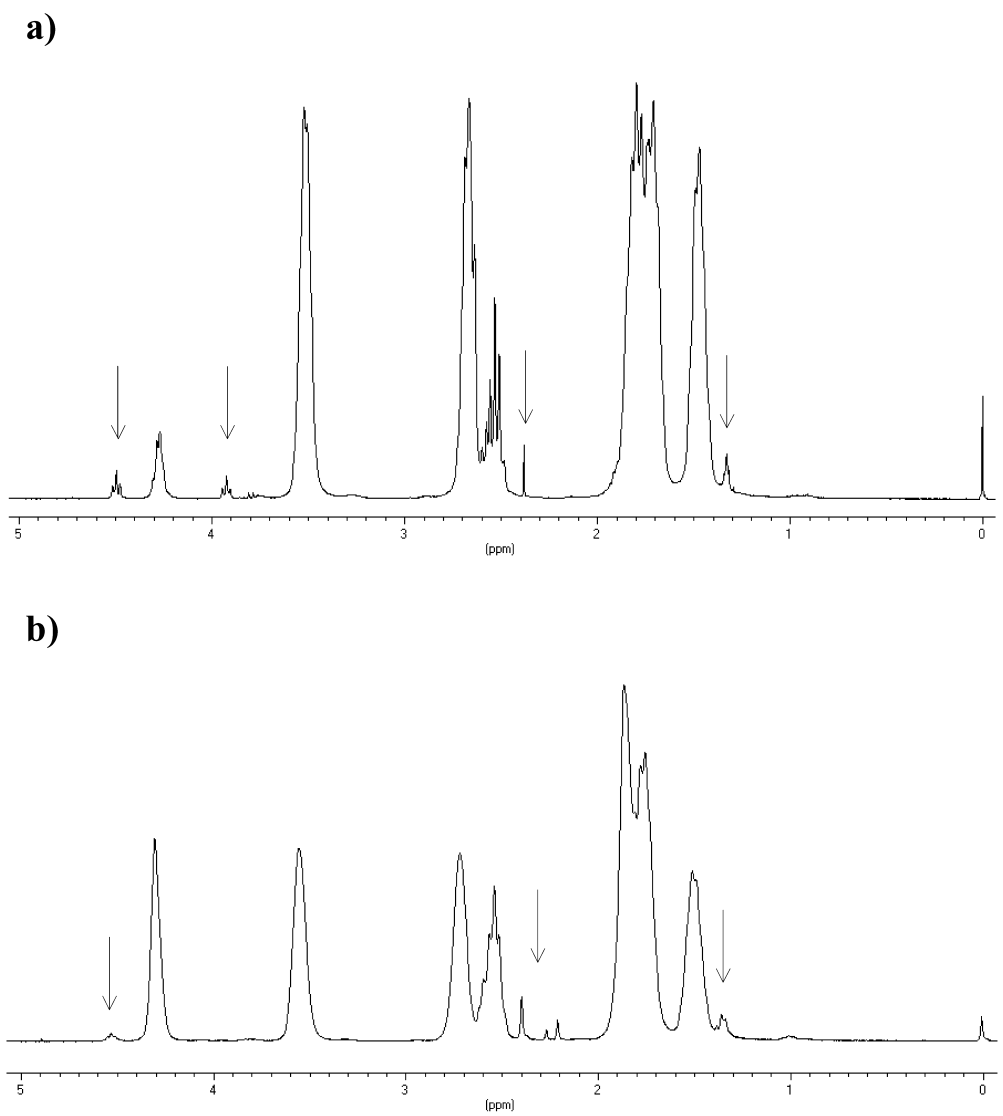

Fig. 8. ^{1}H NMR spectra of BAK 1095 after 150 days of exposure in distilled water at 70 °C (a) and 21 days in a proteinase K medium (b). Arrows indicate peaks associated to terminal groups produced during degradation.

Table 4
Stress–strain parameters of BAK 1095 and PAHBAH4 samples

	BAK 1095		PAHBAH4
	Melt pressed	After 1 day of buffer immersion	Melt pressed
Young's modulus (MPa)	250	130	350
Tensile strength (MPa)	27	17	28
Elongation at break (%)	570	450	510

4.18 and 3.80 Å suggest a stacking of hydrogen bonded sheets with a shift between consecutive layers of 4.79/2 Å. A chain repeat close to 30 Å (a value of 31.2 Å is expected for a fully extended repeat unit) could also be deduced from the 004 and 008 reflections that appear off the meridian, which consequently indicate a non-orthorhombic lattice.

As previously reported, the packing of poly(ester amide)s is a compromise between the different preferences of polyesters and polyamides. Thus, changes in the amide/ester ratio or in sequence distribution may give rise to the different reported fiber diffraction patterns.

3.4. Hydrolytic and enzymatic degradation

Fig. 7 shows the remaining weight percentages (a) and the changes in intrinsic viscosity (b) of BAK 1095 samples after immersion in different media. The results clearly demonstrated that the polymer degrades well, the increase in temperature (from 37 to 70 °C) being the main factor. Thus, viscosity falls to 0.22 dl/g after only 18 days of exposure in distilled water at 70 °C. Evaluation of degradability throughout the determination of the remaining weight is in some cases problematic due to the different solubilization of fragments in degradation media. In this way, samples exposed to a pH 2.3 medium have a higher decrease in intrinsic viscosity than those exposed to a pH 10.5 medium, whereas a lower weight loss is found in the former. The slight synergetic effect of the combination of sludges and water, which is clear from observation of the intrinsic viscosity changes of samples exposed to sludges, water or their combination should also be pointed out.

^{1}H NMR spectra indicate that degradation took place mainly through the cleavage of ester linkages. Note the appearance of new weak signals in the spectrum of Fig. 8(a), which are indicative of hydroxyl terminal groups ($-CH_2OH$ at 3.98 ppm and its trifluoroacetylated form $-CH_2OCOCF_3$ at 4.52 ppm), and the decrease in the area ratio of protons adjacent to the ester groups (both $-CH_2OCO$ at 4.24 ppm and $-CH_2COO$ at 2.48 ppm). Furthermore, the ester/amide ratio could be evaluated during the degradation of the polymers by using the $(A_{4.24} \times 100)/A_{3.52}$ area relationship. Thus, after 50 days of exposure the ester ratio decreased from 40 to 37% (pH 2.4 medium) or 24% (distilled water at 70 °C), whereas a value of 9% was determined after 150 days of exposure in the latter medium (70 °C).

Fig. 9 compares the degradation behavior of BAK 1095 and PAHBAH4 samples in pH 7.4 aqueous media at 37 °C and distilled water at 70 °C. The results clearly indicate that, in spite of its higher ester content, the ordered polymer degrades at a significantly slower rate than the random poly(ester amide) as a consequence of its higher crystallinity (32 versus 14%).

Degradation of BAK 1095 was also studied in different media containing enzymes with estearase (lipases from *P. cepacia*, *C. cylindracea* or *Rhizophus arrhizus*) or protease (papain, proteinase K or chymotrypsin) activity. Table 3

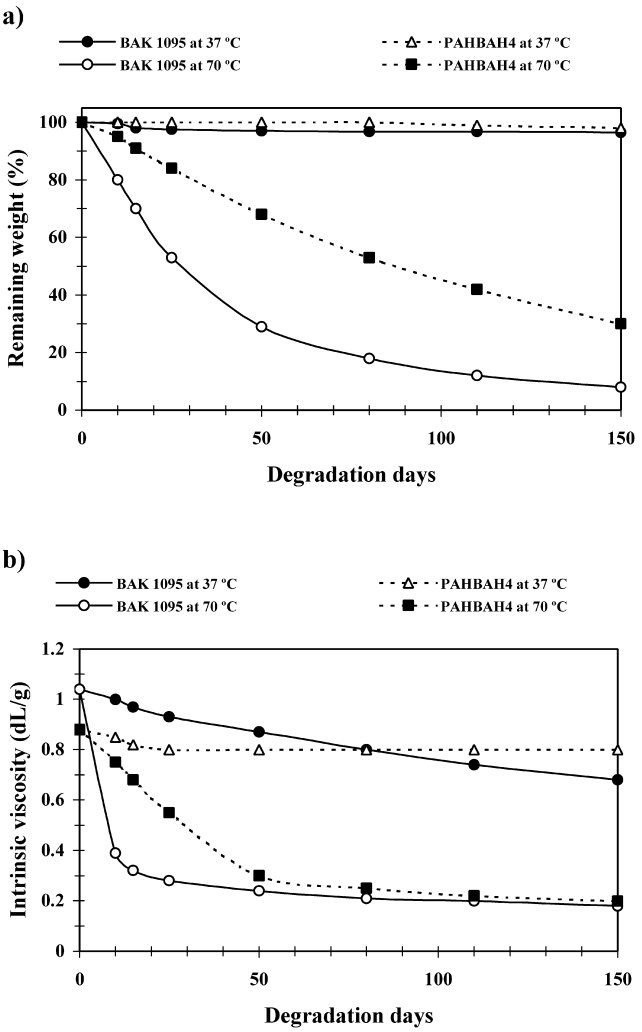

Fig. 9. Remaining weight percentages (a) and intrinsic viscosities (b) of BAK 1095 and PAHBAH4 samples exposed to a pH 7.4 aqueous medium at 37 °C or to distilled water at 70 °C.

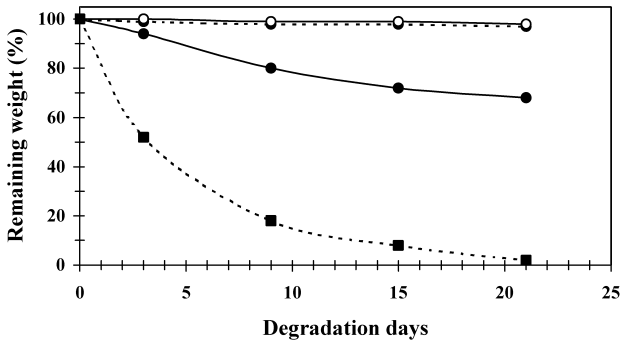

Fig. 10. Remaining weight percentages of BAK (●), PAHBAH4 (○) and polyester 4 6 (■) samples exposed to proteinase K (—) or lipase from *P. cepacia* (- - -) enzymatic media.

demonstrates that proteinase K degrades the polymer well, since a weight loss close to 30% was attained after 21 days of exposure. On the contrary, the stability of the polymer towards the other assayed enzymes is significant, since a weight loss lower than 5% after the same incubation period was found. This fact contrasts with the high susceptibility of polyester 4 6 towards lipase from *P. cepacia*, which produces the total solubilization of the sample after only 21 days of exposure (Fig. 10). Also note that this polyester is stable towards proteases such as the indicated proteinase K, as expected. Another remarkable fact, shown also in Fig. 10, is the low degradability of the PAHBAH4 samples compared with the random BAK 1095 polymer. The different behavior may be a consequence of the lower crystallinity of BAK 1095. It might also be considered that some sequences such as the AH–AH diads are non-existent on the ordered poly(ester amide).

^{1}H NMR spectra of samples exposed to the proteinase K medium show few changes during degradation even though of an appreciable weight loss is attained after only 20 days of incubation. This fact indicates that the enzymes can basically attack only the surface of the samples. However, small peaks indicative of bond cleavages can be detected, as shown in Fig. 8(b).

Scanning electron micrographs are also useful to demonstrate the different surface attacks of the assayed degradation media. Fig. 11 compares hydrolytic degradation at temperatures of 37 and 70 °C for the same exposure time (50 days). The surface remains practically smooth in the first case, whereas numerous holes appear at 70 °C. Micrographs taken at low magnification also reveal the emergence of large, and deep fissures.

Fig. 12 shows how the BAK 1095 is clearly eroded under the attack of proteinase K, increasing the holes size with the exposure time (from 9 to 11 days).

3.4.1. Mechanical properties

Stress–strain data (Table 4) show that the studied poly(ester amide)s have elastic and plastic deformation regions, and that some differences can be detected depending on the sequence distribution, and thus on the

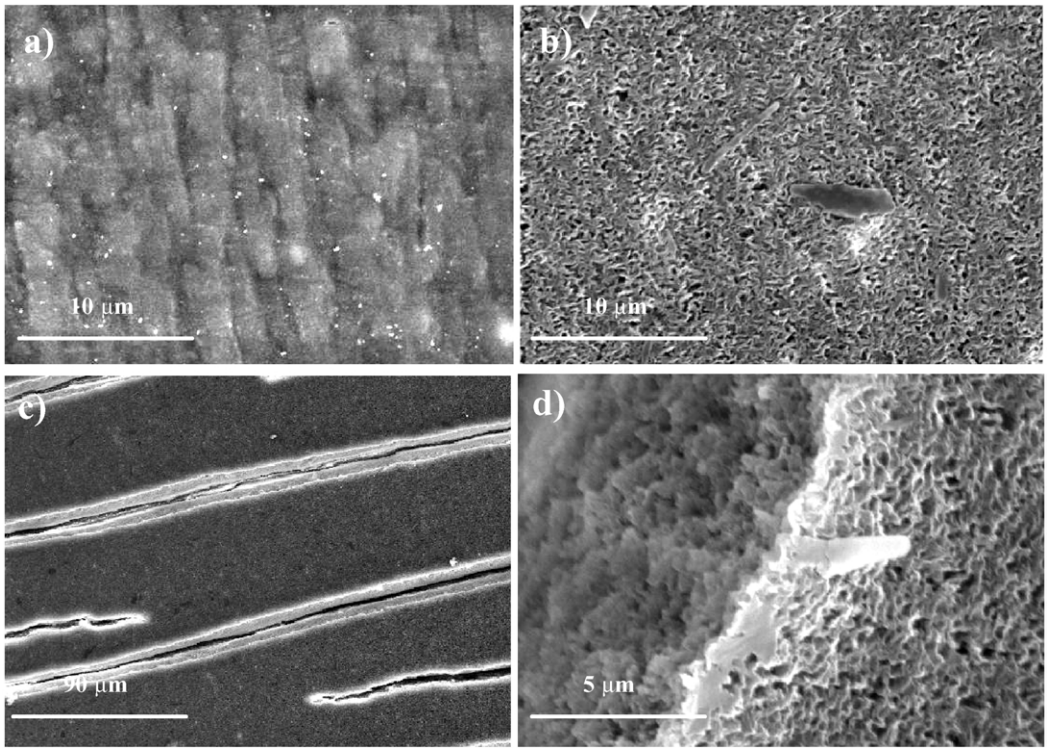

Fig. 11. Scanning electron micrographs of BAK 1095 plates after 50 days of exposure in a pH 7.4 buffer at 37 °C (a) and distilled water at 70 °C (b–d). Note the emergence of deep crevices in the low magnification micrograph (c) of the sample exposed to accelerated degradation conditions. The surface (right) and side (left) of a fissure are shown in the high magnification micrograph (d).

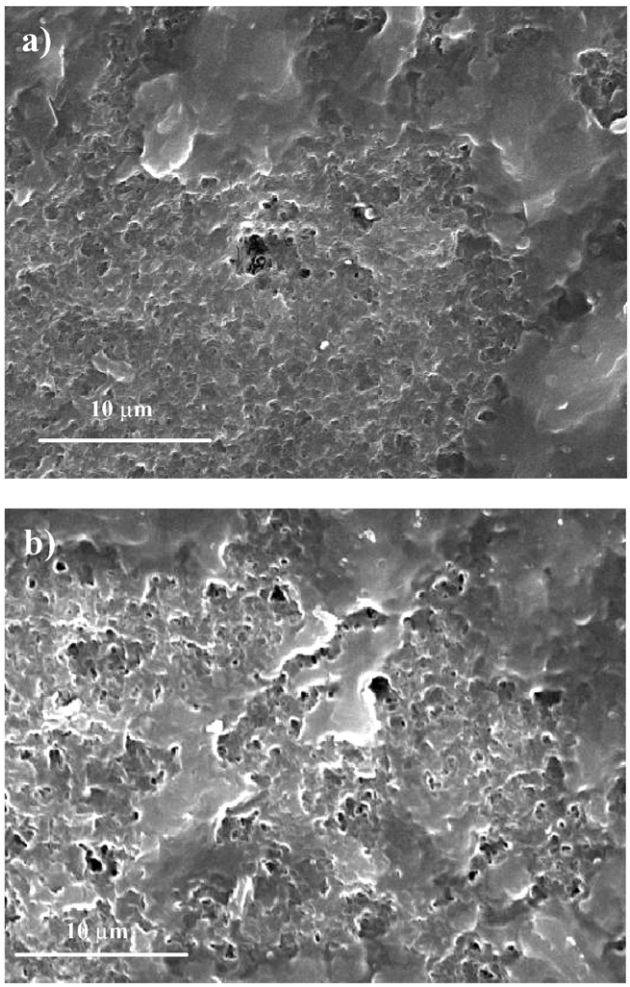

Fig. 12. Scanning electron micrograph of BAK 1095 samples exposed to a proteinase K enzymatic medium for 9 (a) and 21 (b) days. Note that the polymer surface becomes more and more eroded, as shown by the increase in both number and size of pores.

degree of crystallinity. Thus, Young's modulus and tensile strength are higher for the ordered PAHBAH4 sample in spite of its lower amide content. In the same way, elongation at break decreases. The measured values for Young's modulus are characteristic of partially crystalline materials assayed at temperatures above their glass transition temperature.

The mechanical properties depend on the treatment of samples. Thus, for comparative purposes, Table 4 also shows the loss of mechanical parameters after immersing the samples in an aqueous medium for a sufficiently short period of time (1 day) to prevent hydrolytic degradation. The hydrophilic character of BAK 1095 causes the absorption of a non-negligible amount of water, which is clearly manifested by the increase in thickness of the plate samples from the initial value of 200 to approximately 204 μm.

Fig. 13 shows the evolution of the mechanical properties during degradation in different representative media for both dry and wet samples. In general, elongation at break is

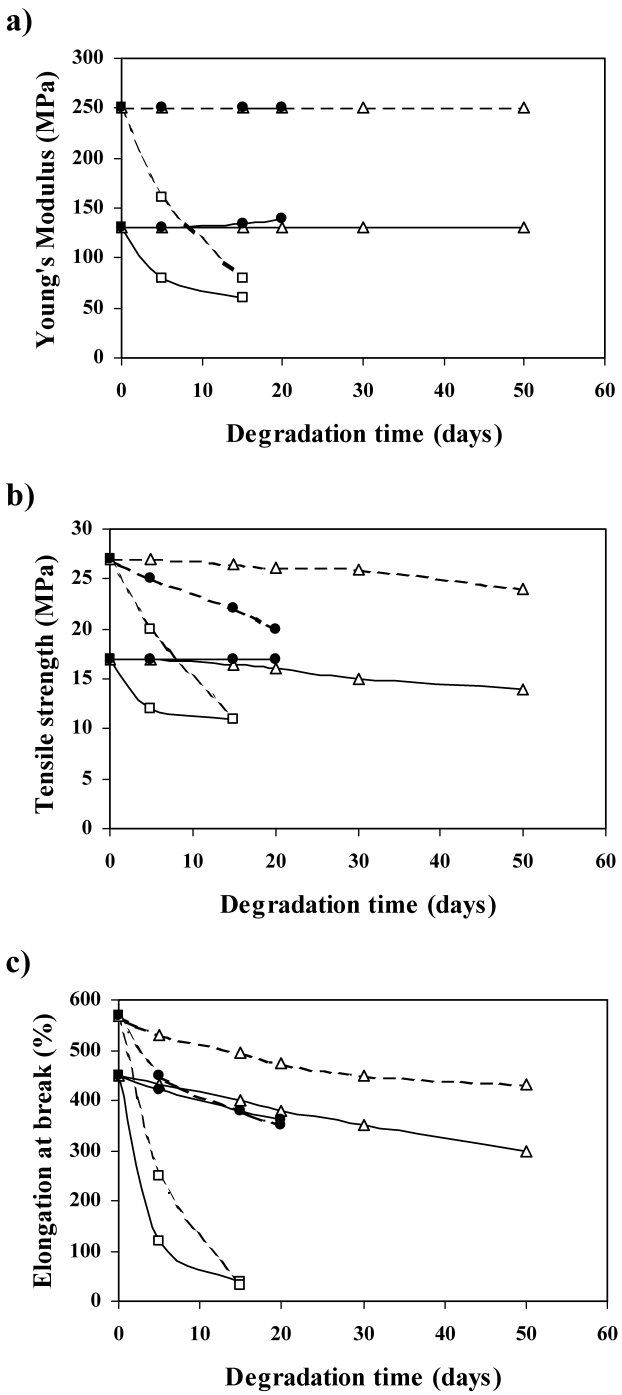

Fig. 13. Changes in the mechanical properties of BAK 1095 versus degradation time for wet (—) and dry (- - -) samples after exposure in a pH 7.4 aqueous medium at 37 °C (△), distilled water at 70 °C (□) and a proteinase K medium (●).

the most sensitive property. Thus, samples exposed to distilled water at 70 °C become breakable to extend the study in this medium for more than 18 days. Some other significant features can be considered:

(a) As discussed above, degradation in the proteinase K medium takes place mainly in the sample surface.

Thus, Young's modulus and tensile strength remain practically constant throughout the study. In addition, the modulus of the wet samples seems to increase slightly. In fact, a gradual slimming of the sample is observed during degradation, and the initial sample thickness of 200 μm is reduced to only 115 μm after 30 days of exposure. This fact makes it impossible to extend measurement of properties for longer periods of time.

(b) Young's modulus and tensile strength also remain practically constant during exposure in a pH 7.4 buffered solution at 37 °C for periods not longer than 50 days. Note, however, that the sample is slightly degraded, as both the loss of intrinsic viscosity (Fig. 7(b)) and the decrease in the elongation at break indicate.

(c) Degradation in distilled water at 70 °C is extremely fast. Thus, a 30–40% decrease for both Young's modulus and tensile strength is detected after only 5 days of exposure. In addition, a 60–70% decrease is observed for elongation at break. Note that a 20% weight loss and an intrinsic viscosity change from 1.04 to 0.70 dl/g are found after a 5 day exposure in this medium (Fig. 9).

4. Conclusions

The results reported in this work can be summarized as follows:

1. The ^{13}C NMR spectrum of BAK 1095 allows its sequence distribution to be analyzed, since different diads and triads can be detected and assigned taking into account the spectra of polyester 4 6, nylon 6 and the poly(ester amide) PAHBAH4 used as reference. BAK 1095 has a statistical distribution of the 1,4-butanediol, 1,6-aminohexanoic acid and adipic acid monomers, obviously considering the chemical bond restrictions. The ^{1}H NMR spectrum of BAK 1095 shows an amide/ester ratio close to 6/4.
2. A sequential poly(ester amide) (PAHBAH4) constituted by the same monomers as BAK 1095 can be synthesized with high yield and intrinsic viscosity by a two-step procedure that involves a final thermal polyesterification.
3. Both BAK 1095 and PAHBAH4 are thermally stable up to temperatures over 100 °C higher than their melting temperatures (138 and 159 °C, respectively). Thus, melt processing is feasible for both poly(ester amide)s. The regular sequence distribution of PAHBAH4 increases its crystallinity and its melting temperature with respect to BAK 1095 in spite of the decrease in its amide content.
4. BAK 1095 can be hydrolytically degraded through ester bond cleavages. The degradation process is clearly accelerated at high temperatures, or in acid or basic pH media. In the same way, the polymer is susceptible to enzymatic attack with proteases such as proteinase K. On the contrary, the sequential PAHBAH4 poly(ester amide) is more stable through both hydrolytic and enzymatic degradation.
5. The mechanical properties of BAK 1095 are highly affected by the degradation process, elongation at break being the most sensitive parameter.

Acknowledgements

This research has been supported by a research grant from CICYT (MAT-2000-0995). We also express our gratitude to Mr Eduardo Ortiz from Bayer Hispania S.A. for his interest and for providing us with the BAK samples, and also to Dr Montse Marsal of the Departament de Materials for the scanning electron micrographs.

References

[1] Grigat E, Koch R, Timmermann R. Polym Degrad Stab 1998;59:223.
[2] Paredes N, Rodríguez-Galán A, Puiggalí J. J Polym Sci, Polym Chem Ed 1998;36:1271.
[3] Paredes N, Casas MT, Puiggalí J, Lotz B. J Polym Sci, Polym Phys Ed 1999;37:2521.
[4] Rodríguez-Galán A, Paredes N, Puiggalí J. Curr Trends Polym Sci 2000;5:41.
[5] Asín L, Armelin E, Montané J, Rodríguez-Galán A, Puiggalí J. J Polym Sci, Polym Chem Ed 2001;4283:39.
[6] Armelin E, Urpí L, Solans X, Puiggalí J. Acta Crystallogr C 2001;57:932.
[7] Karle I, Ranganathan D, Shah K, Vaish NK. Int J Pept Protein Res 1999;43:160.
[8] Alemán C, Navas JJ, Muñoz-Guerra S. J Phys Chem 1995;99:17653.
[9] Van Krevelen DW. Properties of polymers, 3rd ed. Amsterdam: Elsevier; 1990.
[10] Brandrup J, Immergut H. Polymer handbook. New York: Wiley; 1989.
[11] Holmes DR, Bunn CW, Smith DJ. J Polym Sci 1955;17:159.